

Chlorination–Methylation of the Hydrogen-Terminated Silicon(111) Surface Can Induce a Stacking Fault in the Presence of Etch Pits

Santiago D. Solares, Hongbin Yu, Lauren J. Webb, Nathan S. Lewis,* James R. Heath,* and William A. Goddard, III*

Division of Chemistry and Chemical Engineering, California Institute of Technology, Pasadena, California 91125

Received August 15, 2005; E-mail: wag@wag.caltech.edu; nslewis@caltech.edu; heath@caltech.edu

Functionalized Si(111) surfaces have a variety of applications in molecular electronics¹, sensing,^{2–4} photoelectrochemistry,⁵ chemical and electrical surface passivation,^{6,7} porous Si photoluminescence,⁸ and control of photopatterning.⁹ Recently, we demonstrated experimentally that a two-step chlorination–alkylation procedure can achieve 100% coverage of CH₃ on Si(111), leading to complete surface passivation.¹⁰ Characterization with low-energy electron diffraction (LEED) and scanning tunneling microscopy (STM) at 77 K showed a well-ordered 1 × 1 structure for Si(111)–CH₃.¹⁰ The STM images at 4 K revealed that the C–H bonds in the methyl groups are rotated 7° away from the center of the adjacent methyl groups toward an underlying Si atom, giving a H–C–Si–Si torsion angle $\phi = 23 \pm 3^\circ$ (Figure 1). Since the van der Waals repulsions between adjacent methyl groups are lowest for $\phi = 30^\circ$, the experimental result suggests a tendency of the methyl groups toward the *eclipsed* configuration with respect to the surface. Steric interactions between the C–H bonds of methyl and the Si–Si bonds of the top two layers of the surface are expected to lead to a preference for the staggered geometry ($\phi = 60^\circ$). Consequently, we carried out Quantum Mechanics (QM) calculations using the B3LYP and PBE flavors of Density Functional Theory (DFT) and extensive basis sets (Supporting Information section 1) on a series of small molecules, including H₃C–CH₃, H₃Si–SiH₃, H₃C–SiH₃, H₃C–C–(CH₃)₃, H₃Si–Si–(SiH₃)₃, and H₃C–Si–(SiH₃)₃, finding that all prefer strongly the staggered configuration ($\phi = 60^\circ$). Similar level periodic boundary condition DFT calculations using PBE and both plane wave and Gaussian basis sets on Si(111)–CH₃ surface slabs give $\phi = 37.5^\circ$, distorting toward the *staggered* configuration and contradicting the experimental result from the 4 K STM data. Interestingly, the deviation with respect to $\phi = 30^\circ$ is of comparable *magnitude* for theory and experiment, but in the *opposite* direction. The purpose of this work is to demonstrate that the emergence of a stacking fault during the chlorination–alkylation process is energetically favorable and would resolve this discrepancy.

Extracting ϕ from the STM data requires (1) the orientation of the unit cell relative to the overlayer, and (2) the registry of observed spots in the STM image with the atop sites on the Si surface. We believe that the registration of the spots relative to the Si atop sites is robust because the Si–C bond length has been determined independently from photoelectron diffraction measurements to be 1.85 Å.¹¹ The orientation of the lattice planes relative to the imaged STM spots was established by two independent methods.¹⁰ We also verified through DFT calculations that the large electric field present in the STM has a negligible effect on the CH₃ orientation.

Since a single stacking fault between the 1st and 2nd Si layers would have the effect of rotating the apparent torsion of the CH₃ by 60° with respect to the bulk, we carried out DFT calculations with stacking faults on Si(111)–H, Si(111)–Cl, and Si(111)–CH₃ (a more detailed version of this discussion is included in section 5 of the Supporting Information). Indeed with a stacking fault, we found that the *apparent* torsion angle with respect to the bulk would

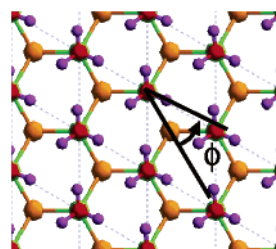


Figure 1. Si(111)–CH₃ surface showing the H–C–Si–Si torsion angle, ϕ , and the hexagonal 1 × 1 unit cell; $\phi = 60^\circ$ is staggered, $\phi = 0^\circ$ is eclipsed, and $\phi = 30^\circ$ minimizes the H···H van der Waals repulsions. Purple = hydrogen, red = carbon, green = first-layer silicon (directly below carbon), and orange = second-layer silicon.

Table 1. Stacking Fault Energy Cost Per Surface Site of Perfect Surfaces, Differential Strain Energy Per Edge Site ($\langle 11\bar{2} \rangle - \langle \bar{1}12 \rangle$), and Equivalent Faulted Sites Per Edge Site Differential Strain^a

surface	$\Delta E_{\text{stacking fault}}^b$ eV/1 × 1 cell	δE_{strain} eV/edge site	equivalent faulted/edge sites ^a
Si(111)	0.048	N/A	N/A
Si(111)–H	0.031	0.05	1
Si(111)–Cl	0.033	0.58	17
Si(111)–CH ₃	0.034	0.67	19

^a Obtained by dividing numbers in the 2nd column by those in the 1st column and meaningful only if $\delta E_{\text{strain}} > 0$ (i.e., favorable stacking fault).

^b The calculated bulk Si value of $\Delta E_{\text{stacking fault}}$ is 0.015 eV/1 × 1 cell.

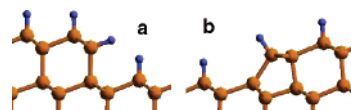


Figure 2. The $\langle 11\bar{2} \rangle$ (a) and $\langle \bar{1}12 \rangle$ (b) step edges for the Si(111)–H surface. The $\langle \bar{1}12 \rangle$ structure (b) has reconstructed to have its substituents perpendicular to the edge surface and to lower its energy.¹²

change from 37 to 23° (there was no effect on the H–C–Si–Si torsion angle). However, the DFT results showed that a stacking fault is *not* favored for any of these perfect surfaces (Table 1, 1st column). Since no other geometrical explanation can reconcile the experimental and theoretical results, we continued to consider how a stacking fault could be stabilized.

Since ~16% of the area on our Si(111)–CH₃ surface was covered by etch pits, we considered whether chemisorbed species on the step edges might stabilize the stacking fault on the terrace. To test this possibility, periodic DFT calculations were performed on Si(111)–H, Si(111)–Cl, and Si(111)–CH₃ models containing an infinite $\langle 11\bar{2} \rangle$ or $\langle \bar{1}12 \rangle$ step edge (Figure 2).¹² The difference in strain between these two step edges was calculated per edge site. The strain energy difference was found to be small for Si(111)–H, but not for Si(111)–Cl and Si(111)–CH₃, which exhibit a strong preference for $\langle \bar{1}12 \rangle$ (Table 1, 2nd column).

To understand these differences, consider first Si(111)–H. Here the Si–Si bond lengths and Si–Si–Si bond angles are close to the

bulk value for $\langle 11\bar{2} \rangle$ (Supporting Information section 4), and all H...H nearest neighbors distances are $>2.97 \text{ \AA}$, causing no significant unfavorable interactions (compare to 2.51 \AA for polyethylene). In contrast, for Si(111)–Cl, some of the nearest neighbor Cl...Cl distances are $\sim 3.23 \text{ \AA}$ for $\langle 11\bar{2} \rangle$, but $>3.84 \text{ \AA}$ for $\langle \bar{1}\bar{1}\bar{2} \rangle$. Since the van der Waals radius of Cl is $\sim 3.95 \text{ \AA}$,¹³ substantial steric repulsions are expected for $\langle 11\bar{2} \rangle$. Indeed the calculations indicate that the Si–Cl bond on $\langle \bar{1}\bar{1}\bar{2} \rangle$ is 0.58 eV stronger than that on $\langle 11\bar{2} \rangle$ (Table 1, 2nd column). The contribution of the *reconstructed* $\langle \bar{1}\bar{1}\bar{2} \rangle$ step edge (Figure 2b) to the energy of the bare Si(111) surface is lower than that of the *unreconstructed* $\langle \bar{1}\bar{1}\bar{2} \rangle$ edge by 0.81 eV/site and lower than that of $\langle 11\bar{2} \rangle$ (Figure 2a) by 0.56 eV/site (Supporting Information section 4). For Si(111)–CH₃, the nearest neighbor H...H distance on $\langle 11\bar{2} \rangle$ is 2.07 \AA (0.44 \AA shorter than in polyethylene!), whereas the shortest distance on $\langle \bar{1}\bar{1}\bar{2} \rangle$ is 2.29 \AA , resulting in a Si–CH₃ bond with significantly lower strain energy on $\langle \bar{1}\bar{1}\bar{2} \rangle$ than on $\langle 11\bar{2} \rangle$ (by 0.67 eV).

The samples in the 4 K STM experiments used the Si(111)–H surface as an intermediate step in preparing the methylated surface. The step edges around the etch pits were verified to be in the $\langle 11\bar{2} \rangle$ family, and their orientation did not change during the subsequent chlorination and alkylation steps (using PCl₅ and CH₃MgCl in THF).¹⁰ Hence, relief of the strain for Si(111)–Cl and Si(111)–CH₃ through the formation of the more favorable step edge termination shown in Figure 2b requires the introduction of a stacking fault between the 1st and 2nd Si layers *on the terraces* [note that when the step edge orientation is $\langle 11\bar{2} \rangle$, the *normal* crystal has the structure in Figure 2a, while the *faulted* crystal has the structure in Figure 2b]. Taking the difference in strain energy between the two types of step edges as the driving force for the formation of the stacking fault, and dividing this by the stacking fault energy cost, yields the number of equivalent faulted sites (Table 1, 3rd column) that this strain energy is able to induce (neglecting the energy of the rows of Si dimers at the borders between faulted and unfaulted regions¹²). Thus, allowing one edge site to transform from the structure of Figure 2a to that of Figure 2b would compensate for ~ 17 *faulted* sites on Si(111)–Cl and for ~ 19 *faulted* sites on Si(111)–CH₃. This ratio is greater than the ratio of terrace to edge sites on the experimental Si(111)–CH₃ surface (~ 13), indicating that a full stacking fault on the terraces is energetically possible.

The theory-derived conclusion that there is a stacking fault in the Si(111)–CH₃ surface is consistent with the STM experiments of Ithckawitz et al.,¹² who observed stacking faults on terrace regions adjacent to $\langle 11\bar{2} \rangle$ steps on Si(111)–Cl. They did *not* observe full stacking faults, but with their method (exposure of a DAS 7×7 Si(111) surface to Cl₂ gas at $673\text{--}773 \text{ K}$), the $(7 \times 7) \rightarrow (1 \times 1)$ transformation occurs predominantly along step edges.¹² In some cases, they may have also examined the surface structure before it transformed fully into a 1×1 Si(111)–Cl. Since the CH₃–MgCl Grignard reagent in our experiments is appreciably larger than Cl₂, it is plausible that steric interactions would play an even more significant role in the formation of a stacking fault in our Si(111)–CH₃ samples.

The Si(111)–CH₃ surfaces were prepared at THF reflux temperature ($\sim 65 \text{ }^\circ\text{C}$), at which Si(111) surface reconstructions do *not* occur spontaneously, but we believe they could be induced to accommodate the sterically hindered transition states expected for the Grignard conversion of the Cl surface to the CH₃ surface. This process is very exothermic (DFT leads to $\Delta G^{298^\circ} = -41.0 \text{ kcal/mol}$, after including solvation using the Poisson–Boltzmann continuum model), so that the local temperature may increase the mobility of the atoms on the surface.

The emergence of a stacking fault during the chlorination–alkylation of Si(111)–H to produce Si(111)–CH₃ would resolve the discrepancy between theory and experiment. Thus the experi-

mental torsion angle of 23° with respect to the bulk crystal would correspond to 37° with respect to the second Si layer on the terraces. On the other hand, the calculations indicate that the CH₃ groups in the etch pits would have the normal angle of 37.5° with respect to the bulk. Measuring this would provide an excellent validation of the model, but current low-temperature STM experiments can only observe the top layer.¹⁰

Despite the consistency of our stacking fault model in explaining the apparent discrepancy between theory and experiment, some questions remain. The theory suggests that there would *not* be a stacking fault if there were no etch pits. Currently, the best experimental surfaces exhibit etch pits and step edges, and it is not clear whether unfaulted Si(111)–CH₃ surfaces can be produced through chlorination–alkylation methods or by different synthetic routes. Also, we have not yet predicted the reaction barriers for the formation of stacking faults on the terraces. Hence, our estimate of the ratio of faulted sites to edge sites is an upper bound. We have also not examined whether the methylation process starts at the edges at already faulted sites and propagates toward the terraces, or occurs randomly on the terraces and edges simultaneously. Experimental studies using LEED to examine the orientation of the etch pit CH₃ and STM studies of asymmetric substituents on Si(111) (such as CH₂F) might test our predictions. In addition, theoretical study of the reaction barriers for the chlorination–methylation would provide more insight into the formation mechanism, structure, and energetics of the Si(111)–CH₃ surface.

Summarizing, we use QM to show that in the presence of etch pits the introduction of a CH₃ on each surface Si can induce the formation of a stacking fault between the 1st and 2nd Si layers. This would explain the unexpected experimental CH₃ torsion angle of 23° , reconciling it with the theoretical value of 37.5° . Thus the experimental value of 23° measured with respect to the bulk crystal would correspond to 37° with respect to the 2nd Si layer.

Acknowledgment. Support for S.D.S. and W.A.G. was provided by NSF-CCF-05204490 and by the Microelectronics Advanced Research Corporation (MARCO) and its Focus Center on Function Engineered NanoArchitectonics (FENA). Support for L.J.W. and N.S.L. was provided by NSF-CHE-0213589. Support for H.Y. and J.R.H. was provided by the DOE and NSF-CCF-05204490.

Supporting Information Available: Computational methods, torsional barriers, geometry of Si(111)–CH₃, strain and geometry of $\langle 11\bar{2} \rangle$ and $\langle \bar{1}\bar{1}\bar{2} \rangle$ steps, and detailed stacking fault discussion. This material is available free of charge via the Internet at <http://pubs.acs.org>.

References

- (1) Yates, J. T. *Science* **1998**, *279*, 335–336.
- (2) Pike, A. R.; Lie, L. H.; Eagling, R. A.; Ryder, L. C.; Patole, S. N.; Connolly, B. A.; Horrocks, B. R.; Houlton, A. *Angew. Chem., Int. Ed.* **2002**, *41*, 617–617.
- (3) Strother, T.; Cai, W.; Zhao, X. S.; Hamers, R. J.; Smith, L. M. *J. Am. Chem. Soc.* **2000**, *122*, 1205–1209.
- (4) Lin, Z.; Strother, T.; Cai, W.; Cao, X. P.; Smith, L. M.; Hamers, R. J. *Langmuir* **2002**, *18*, 788–796.
- (5) Bansal, A.; Lewis, N. S. *J. Phys. Chem. B* **1998**, *102*, 4058–4060.
- (6) Bansal, A.; Li, X.; Yi, S. I.; Weinberg, W. H.; Lewis, N. S. *H. Phys. Chem. B* **2001**, *105*, 10266–10277.
- (7) Webb, L. J.; Lewis, N. S. *J. Phys. Chem. B* **2003**, *107*, 5404–5412.
- (8) Song, J. H.; Sailor, M. J. *Comments Inorg. Chem.* **1999**, *21*, 69–84.
- (9) Buriak, J. M. *Chem. Rev.* **2002**, *102*, 1271–1308.
- (10) Yu, H.; Webb, L. J.; Ries, R. S.; Solares, S. D.; Goddard, W. A., III; Heath, J. R.; Lewis, N. S. *J. Phys. Chem. B* **2005**, *109*, 671–674.
- (11) Terry, J.; Linford, M. R.; Wigren, C.; Cao, R. Y.; Pianetta, P.; Chidsey, C. E. D. *Appl. Phys. Lett.* **1997**, *71*, 1056–1058.
- (12) Itchkawitz, B. S.; McEllistrem, M. T.; Boland, J. *Phys. Rev. Lett.* **1997**, *78*, 98–101.
- (13) Mayo, S.; Olafson, B.; Goddard, W. A., III. *J. Phys. Chem.* **1990**, *94*, 8897–8909.

JA055408G